Modulation of the Rate of Electron Injection in Dye-Sensitized Nanocrystalline TiO₂ Films by Externally Applied Bias

Yasuhiro Tachibana,[†,§] Saif A. Haque,[†] Ian P. Mercer,[†] Jacques E. Moser,[‡] David R. Klug,[†] and James R. Durrant*,[†]

Department of Chemistry, Imperial College, London SW7 2AY, U.K., and Institut de Chimie Physique, École Polytechnique Fédérale de Lausanne, CH-1015 Lausanne, Switzerland

We present a study of the kinetics of electron injection in ruthenium(II) *cis*-(2,2′-bipyridyl-4,4′-dicarboxylate)₂-(NCS)₂-sensitized nanocrystalline TiO₂ films as a function of electrical potential applied to the TiO₂ film and as a function of the composition of the electrolyte in which the film is immersed. At moderate applied potentials (−0.2 V vs Ag/AgCl), and in the presence of potential determining ions (0.1 M Li⁺) in the electrolyte, the electron injection kinetics were found to be multiphasic, with a half time for electron injection of 500 fs. These injection kinetics were retarded by either the omission of potential determining ions or the application of more negative potentials. Omission of Li⁺ ions from the electrolyte resulted in a 7-fold retardation of the injections kinetics. The application of −0.7 V to the TiO₂ electrode resulted in a 25-fold retardation of the injection kinetics. These observations are discussed in terms of nonadiabatic interfacial electron transfer theory. The retardation of the injection kinetics in the absence of potential determining ions is attributed to the influence of these ions upon the electronic density of states of the TiO₂ electrode. The retardation of the injection kinetics at negative applied potentials is attributed to the increased occupancy of this density of states. Fits to the potential dependence of the injection kinetics following nonadiabatic theory yield a reorganizational energy for the electron injection process of 0.25 ± 0.05 eV.

Introduction

Wide band gap semiconductors can be sensitized to visible light by the adsorption of molecular dyes to their surface. Attention has particularly focused upon the sensitization of nanocrystalline semiconductors, as their high internal surface area yields a high dye optical density for only monolayer dye coverage. Such dye-sensitized nanocrystalline films, and in particular nanocrystalline TiO₂ films, are now attracting widespread technological interest, particularly in the development of photoelectrochemical solar cells.[1,2]

The kinetics of interfacial electron transfer between the adsorbed sensitizer dye and the semiconductor electrode play in key role in controlling the efficiency of dye-sensitized photoelectrochemical cells. In particular, such devices require a rapid electron injection from the photogenerated dye excited state into the semiconductor conduction band in order to avoid wasteful decay pathways from this excited state (e.g., radiative and nonradiative decay). Interfacial electron transfer kinetics have been traditionally studied by electrochemical techniques[3] which, although powerful, are typically limited to millisecond time resolutions. However the high optical density of dye-sensitized, nanocrystalline films, critical to their technological applications, has the additional advantage of allowing these kinetics to be probed by transient optical spectroscopies, thus allowing the use of the much faster time resolutions achieved with such techniques. Indeed several groups have now employed ultrafast laser spectroscopies to resolve electron injection processes in dye-sensitized nanocrystalline metal oxide films on picosecond and femtosecond time scales.[4−11] Developing a theoretical understanding of such ultrafast electron injection processes is not only of interest scientifically, but likely to be important in technological applications of such sensitized films. In particular it is of interest to determine whether theoretical descriptions of interfacial electron-transfer developed in the 1960s and tested against relatively slow time scale electrochemical measurements[3] can also be applied to such ultrafast electron-transfer reactions, or whether new theoretical models are required.[12,13]

Following theoretical treatments of interfacial electron-transfer processes developed in the 1960s, the rate of electron injection from the excited state of an adsorbed dye molecule into the conduction band of an electrode can be expressed as[3]

$$k_{inj} = A \int V^2 (1 - f(E,E_F)) g(E) \exp\left(\frac{-(E_m - E + \lambda)^2}{4\lambda k_B T}\right) dE \quad (1)$$

where k_{inj} is the electron injection rate, V is the electronic coupling between the dye excited state and each conduction band state of the electrode (assumed to be state independent), and E_m is the excited-state oxidation potential energy of the adsorbed molecule, as illustrated in Figure 1. E is the electrochemical potential energy of conduction band states. The equation corresponds essentially to an extension of Marcus nonadiabatic electron transfer theory by incorporating a continuum of electronic states in the semiconductor. $g(E)$ is the normalized density of states of this conduction band, $f(E,E_F)$ is the Fermi occupancy factor to account of the fact that electron

Electron Injection in Dye-Sensitized TiO$_2$ Films
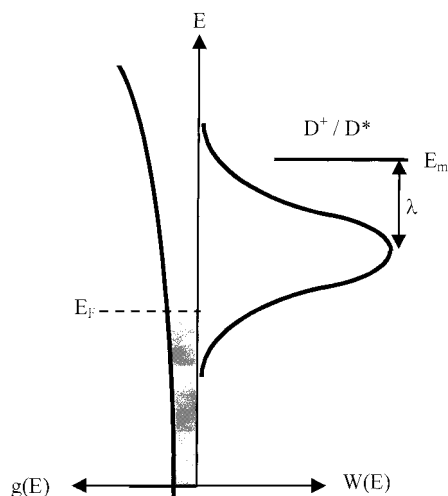
J. Phys. Chem. B, Vol. 105, No. 31, 2001 **7425**

Figure 1. Diagramatic illustration of eq 1. Electron injection from the dye excited state, D*, into semiconductor states of energy E depends on the density of semiconductor states at this energy, $g(E)$, their occupancy determined by the position of the Fermi level, E_F, and the magnitude of the exponential term $W(E)$. $W(E)$ is optimum for semiconductors states of energy $E_m - \lambda$, where E_m and λ are the dye excited-state oxidation potential and the reorganizational energy, respectively. Note E is defined as an electrochemical potential, and therefore E_m is therefore negative.

injection is only possible into unoccupied states. The exponential term, labeled $W(E)$ in Figure 1, accounts for the effective activation barrier to electron injection into a state of energy E, as derived by Marcus and co-workers for homogeneous electron transfer. λ is the reorganizational energy associated with electron injection. From this equation it is apparent that electron injection occurs optimally to conduction band states lying λ below the dye excited-state energy (i.e., when $W(E)$ is maximal). A central prediction of this equation is that as the Fermi level of the semiconductor is raised to an energy within $\sim\lambda$ of the dye excited-state oxidation potential, the rate of electron injection is retarded. This retardation arises from the reduction in unoccupied acceptor states available for electron injection.

Determination of the dependence of the rate of electron injection upon semiconductor Fermi level is of particular relevance to dye sensitized photoelectrochemical solar cells, as the voltage output of such devices derives from the raising of the semiconductor Fermi level induced by solar illumination. However, studies of this dependence to date have been largely based upon steady-state studies of dye photoluminescence under applied electrical bias. An increase in photoluminescence intensity is typically observed upon the application of a negative electrical bias to the semiconductor electrode and attributed to a retardation of the electron injection process.[14] Such studies have recently been supported by ultrafast studies singlet state lifetimes for 5 SnO$_2$ electrodes over a limited bias range.[15] However, it has recently been reported, on the basis of quartz microbalance data, that increases in luminescence intensity under applied bias may also derive from desorption of the dye from the semiconductor surface.[16] Moreover our own studies (I. Montanari, J.R.D., D.R.K., unpublished results) have indicated that the emission decay kinetics are highly heterogeneous, with the slower phases, corresponding to a sub-population of more slowly injecting sensitizer dyes, being most sensitive to applied bias. It is thus clearly desirable to conduct more direct studies of the Fermi level dependence of the injection kinetics.

In addition to the position of the Fermi level, the rate of electron injection is also dependent upon the electronic density of states, $g(E)$. Experimental studies of this density of states

for nanocrystalline TiO$_2$ are at present controversial. Such studies have been largely based by spectroelectrochemical studies of the density of conduction band/trapped electrons induced by electrical bias,[17] complimented more recently by a range of electrochemical techniques.[17-21] These studies have generally concluded that such films exhibit an exponential tail of states below the conduction band, attributed variously to defect states such as oxygen vacancies, surface states, and/or states induced by proton or lithium cation surface binding or intercalation into the TiO$_2$ nanoparticles. The energetics of this density of states has moreover been found to be strongly dependent upon the electrolyte composition, and in particular the concentration of small cations in this electrolyte. Spectroelectrochemical studies have demonstrated that the flat band potential of such films can shift by over one volt depending upon the presence in the electrolyte of "potential determining" cations such as protons or Li$^+$ ions.[17,22] Such ions may or may not also influence the redox properties of the adsorbed sensitizer dye.[23,24] Li$^+$ ions are routinely added to the electrolyte of 5 nanocrystalline photovoltaic devices, as they have been shown to result in improved device performance. The yield of electron injection in 5 nanocrystalline TiO$_2$ films has recently been shown to be sensitive to the concentration of potential determining ions in the electrolyte.[25] This observation was attributed to the influence of such ions upon the electron injection kinetics. In this paper, we extend such studies by direct measurement of these kinetics as a function of ion concentration.

We have demonstrated that following photoinduced electron injection, the kinetics of charge recombination between titania conduction band/intraband electrons and the photoinduced dye cations are strongly dependent both upon the Fermi level of TiO$_2$ and the composition of the electrolyte employed.[26,27] For example, in an ethanolic electrolyte, variation in the applied potential from 0 V to -0.6 V (vs Ag/AgCl) resulted in an acceleration of the recombination reaction from $\sim$1 ms to $\sim$100 ps. This strong dependence upon applied bias has been successfully modeled as a random walk between an exponential energetic distribution of trap sites,[28,29] which predicts a strongly nonlinear dependence of the recombination time upon electron density, as observed experimentally. The strong dependence of the recombination time upon electrolyte composition (up to a factor of 10^6) has been successfully correlated with variations in $g(E)$ probed (albeit indirectly) by spectroelectrochemical studies. In this paper we extend such studies to the dependence of electron injection kinetics in RuL$_2$(NCS)$_2$-sensitized TiO$_2$ nanocrystalline films upon the electrolyte composition and the electrical potential applied to the TiO$_2$ film.

Materials and Methods

Sample Preparation. The preparation of anatase nanocrystalline TiO$_2$ films (average particle diameter: 15 nm and film thickness: 8 μm) and the sensitization of these films with the ruthenium dye, ruthenium(II) *cis*-(2,2′-bipyridyl-4,4′-dicarboxylate)$_2$(NCS)$_2$ (RuL$_2$(NCS)$_2$) were conducted as described previously.[11,26] RuL$_2$(NCS)$_2$ was chosen as it is the sensitizer dye currently most widely used in 5 photoelectrochemical cells. For optical experiments under externally applied bias, the TiO$_2$ film was incorporated as the working electrode of a three-electrode photoelectrochemical cell, which also comprised a platinum wire counter electrode and an Ag/AgCl reference electrode.[26] Acetonitrile (Fluka GLC grade) as the electrolytic solvent was dried by distillation over CaH$_2$ prior to use. All electrolytes were degassed with argon prior to and during all optical experiments. Spectroelectrochemical measure-

ments were conducted by placing the photoelectrochemical cell in a Shimadzu UV-1601 absorption spectrometer; further details are given elsewhere.[27]

Femtosecond Transient Absorption Spectrometer. A home-built Ti:sapphire chirped pulse amplifier (CPA) laser system generated ~30 fs pulses (fwhm) with a pulse energy of 350 μJ at 810 nm. Tunable excitation pulses were generated with a home-built optical parametric amplifier (OPA). These fundamental pulses are split into 3 parts by a wedged glass (separation angle: 30 min) plate. 4% of fundamental pulses is used to generate a white light continuum in a 1-cm path length cuvette as probe pulses for the transient absorption spectroscopy and another 4% to generate a white light continuum in a 2-mm path water cell as seed pulses for the OPA. The rest of fundamental pulses were frequency-doubled centered at 405 nm to pump the OPA. Second harmonic conversion was achieved in 1 mm thick Type-I BBO crystal with conversion efficiency of 10% to keep good beam quality. Parametric amplification was operated with 2 stages, for both of which Type I BBO crystals were used. In each stage signal and pump pulses are matched noncollinearly with the crossing angle of approximately 3°. The OPA pulses are compressed by a pair of prisms (SF10). The compressed OPA pulses finally produce ~30 fs pulses with 60~80 nJ in a range of 450~750 nm. For pump−probe experiments, the generated white light continuum of probe pulses is compressed to compensate group velocity dispersion.

Data were collected with the magic angle configuration (ca. 54.7°) between pump and probe pulse polarizations with a repetition rate of 1 kHz at 20 °C. Samples were excited with a pulse energy of 40~50 nJ (0.8~1 mJ/cm^2) at 623 nm, corresponding to the low energy absorption tail of the RuL$_2$-(NCS)$_2$ sensitizer dye (absorbance: 0.07~0.08). We have shown previously that the injection kinetics are independent of excitation wavelength.[30] The number of injected electrons per nanoparticle were estimated both by determination of the number of excited dye molecules per unit area (assuming unity electron injection yield as determined previously), and by assessment of the number of dye cation molecules per unit area following the magnitude of the dye ground-state absorption bleach resulting from cation formation (employing a difference extinction coefficient at 540 nm of 12000 M^{-1} cm^{-1} obtained from previously published data[6]). The number of nanoparticles in 1 cm^2 of the film was calculated with an average TiO$_2$ particle diameter of 15 nm and a film thickness of 8 μm. These two methods yielded indistinguishable injection densities within experimental uncertainties (±40%). All transient experiments employed excitation densities corresponding to ≤1.1 ± 0.3 excited dye molecule/nanoparticle, at a repetition rate of 500 Hz. The stability of all samples was monitored by the change of the signal size during all of transient absorption experiments and by the change of the ground state absorption maximum before and after the transient absorption experiments. No sample degradation was observed, except following the application of strongly negative biases (see below for details).

The instrument response (10~90% rise time of transient absorption changes) of the spectrometer was 100−250 fs determined with dye standards (Nile Blue in methanol and ZnTCPP in ethanol) for probe wavelengths between 680 and 770 nm. Transient absorption data were collected with a multichannel detector, and globally analyzed assuming multiexponential kinetics as described previously.[6] The amplitudes of electron injection associated with each kinetic component were obtained from such global analyses.

Nonadiabatic calculations of the rate of electron transfer followed eq 1. Fitting parameters were λ, E_m, and the preintegral constant, A. An uncertainty in applying eq 1 concerns the form of $g(E)$. For simplicity, the calculations shown employed a constant density of states (i.e., independent of E and E_F). Experimental studies of electron occupancy as function of electrical applied bias suggest, albeit indirectly, that $g(E) \propto \exp(-E/E_0)$, with values of the energy coefficient E_0 varying between 60 and 200 mV between experimental studies.[19,20,28,29] Fits were calculated to the experimental injection data for a range of different values of E_0. It was found that good fits could be obtained to the experimental data for values of $E_0 \geq 100$ mV; moreover after normalization of $g(E)$, the fit parameters E_m and λ were only weakly dependent upon E_0 over this range, being the same within error as those obtained for a constant density of states. This limit corresponds to the range where the potential energy dependence of $W(E)$ is stronger than that of $g(E)$, and therefore the detailed form of $g(E)$ is relatively unimportant. It has also been suggested, due to "band edge unpinning", that $g(E)$ is a function of the applied voltage E_F.[31] We note that such a model, in which the conduction band edge shifts in energy with the applied fermi level, would have the effect of shifting the range of integration of the integral in eq 1. Calculations based upon this model, assuming a constant density of states above the conduction band edge, yielded similar fits, with similar values of the fit parameters E_m and λ to those assuming $g(E)$ to be independent of applied fermi level. We conclude that the potential dependence of the fits were not strongly dependent upon the form of normalized $g(E)$ used; for this reason the fit shown was obtained assuming $g(E)$ to be independent of E_F and in the limit of large E_0, corresponding to an energy independent density of states.

Further calculations were performed to address the potential impact of reverse electron transfer processes back to the dye excited state. Calculations were only conducted for $E_F - E_m \gg k_B T$, and therefore reverse reactions from thermalized electrons could be neglected. Reverse electron transfer, k_{-et}, from injected electrons prior to relaxation down to the Fermi level was considered, with the rate being determined from simple consideration of detailed balance between the injected electron energy, E, and E_m ($k_{-et} = k_{et} \exp(-(E - E_m)/k_B T)$). However, inclusion of this reverse reaction, at least for calculations assuming a constant density of states, had no effect within experimental error on the fit results.

Results

We have previously shown that electron injection in RuL$_2$-(NCS)$_2$-sensitized TiO$_2$ films can be readily monitored by absorption changes in the near-infrared (700−800 nm).[6] Absorption changes in this spectral region are dominated by induced absorption by the sensitizer dye excited and cation states, and most probably arise from a ligand-to-metal charge-transfer transition from the (NCS)$^-$ groups to the Ru^{3+} metal center of the dye excited/cation states.[32] Formation of the RuL$_2$-(NCS)$_2$ excited-state results in induced absorption with a maximum at ~720 nm. For the RuL$_2$(NCS)$_2$ cation state this induced absorption maximum increases in magnitude and shifts to 800 nm.[6,32] Electron injection from the dye excited state to the state (dye$^+$e$_{sc}^-$) can therefore be monitored by time resolving the increase in magnitude of this induced absorption and/or its red shift from 720 to 800 nm. Induced absorption associated with the injected electrons (e$_{sc}^-$) may also contribute to the induced absorption of the sensitized TiO$_2$ films in this spectral window, but is weak relative to the dye cation absorption, and cannot be distinguished from it.[6]
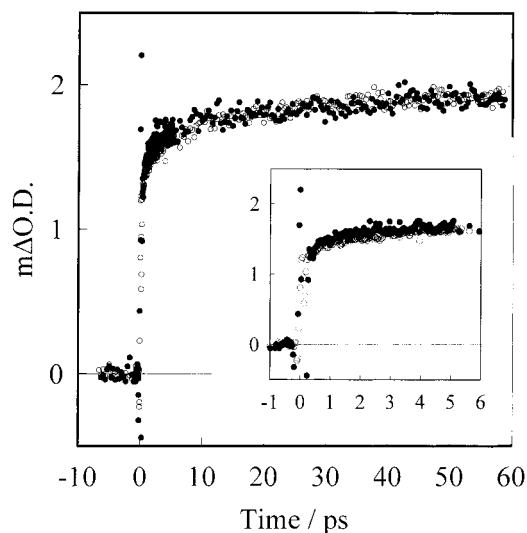
Electron Injection in Dye-Sensitized TiO$_2$ Films

J. Phys. Chem. B, Vol. 105, No. 31, 2001 **7427**

Figure 2. Comparison of the electroninjection kinetics for RuL$_2$(NCS)$_2$-sensitized TiO$_2$ films collected in the absence (●) and the presence (○) of externally applied bias. Data shown are transient absorption kinetics collected at a probe wavelength of 760 nm following excitation at 623 nm. Data in absence of applied bias (●) were collected for films covered in propylene carbonate/ethylene carbonate as previously reported.[11] Data in the presence of applied bias (○) was collected in a three-electrode photoelectrochemical cell, employing a LiClO$_4$/MeCN electrolyte (electrolyte A) at an applied bias of −0.2 V vs Ag|AgCl. Oscillatory signals near zero time delay result from impulsive stimulated Raman scattering in the glass substrate.

In this paper we consider the influence of electrolyte composition and externally applied electrical bias upon the kinetics of electron injection. Our previous studies have been limited to RuL$_2$(NCS)$_2$ films in the absence of applied bias covered in a range of solvents (ethylene carbonate/propylene carbonate (EC/PC) and ethanol) or exposed to air.[6,11,30] Here we extend these studies by incorporating the sensitized TiO$_2$ film as the working electrode of a three-electrode photoelectrochemical cell, and employing an anhydrous electrolyte with and without the addition of a high concentration of potential determining ions. The electrolytes employed were 0.1 M tetrabutylammonium perchlorate (TBAP) in anhydrous acetonitrile with (A) and without (B) the addition of 0.1 M lithium perchlorate (LiClO$_4$).

Spectroelectrochemical studies of unsensitized TiO$_2$ electrodes indicated that the addition of 0.1 M LiClO$_4$ resulted in positive shift of approximately one volt in the potential dependence of the electron occupancy of conduction band/trap states, observed as a blue/black coloration of the film attributed to Ti^{3+} states, indicative of a ∼1 V shift in the density of states $g(E)$. This shift is likely to be significantly less for sensitized films, due to the presence of protons deriving from the carboxylic acid moieties of the sensitizer dye. Studies of sensitized films could only be conducted over a more limited voltage range in order to avoid irreversible reduction/degradation of the sensitizer dye. Such studies of sensitized films indicated a shift of the spectroelectrochemical signal by ≥300 mV between the two electrolytes.

Figures 2 and 3 show transient absorption kinetics at a single probe wavelength, 760 nm, indicative, as discussed above, of electron injection from the RuL$_2$(NCS)$_2$ excited state into TiO$_2$. Figure 2 shows a comparison of data collected in electrolyte A under a moderate applied potential (−0.2 V vs Ag/AgCl, see below) with previously published data collected in the absence of applied bias.[30] Figure 3 shows a comparison of data collected at −0.2 V for electrolytes A and B (circles and triangles,
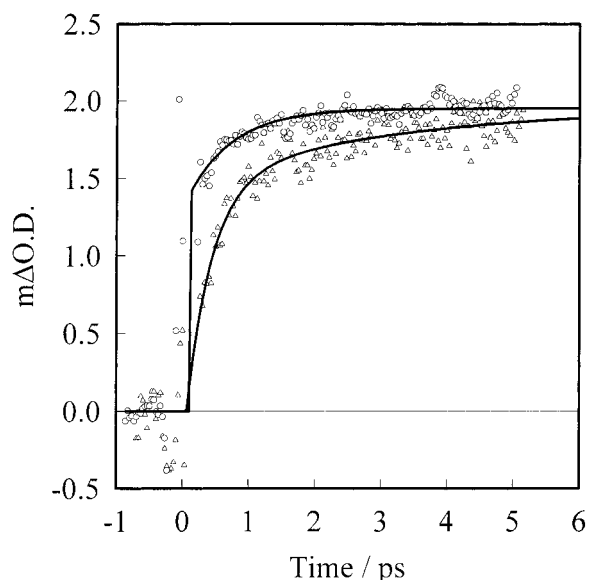

Figure 3. Transient absorption data for RuL$_2$(NCS)$_2$-sensitized TiO$_2$ films collected in the presence (circle) and the absence (triangle) of Li$^+$ in the electrolyte (electrolytes A and B, respectively) with a probe wavelength of 760 nm. The experimental conditions were the same as those presented in Figure 2 at an applied bias of −0.2 V versus Ag|AgCl. Results of the kinetic fitting are shown as solid lines.

respectively). As illustrated in Figure 2, the electron injection kinetics obtained in electrolyte A are indistinguishable from those obtained previously in the absence of applied bias in a range of different solvents,[6,30] requiring a minimum of three components to fit the injection kinetics, with lifetimes (relative amplitudes) of <150 fs (0.4 ± 0.05), 850 ± 250 fs (0.28 ± 0.05), and 15 ± 3 ps (0.32 ± 0.05). Assignment of these components to electron injection was confirmed from amplitude spectra which determined that all three components was associated with red shifts of the near-infrared photoinduced absorption maximum characteristic of electron injection, as discussed previously.[6]

Determination of the proportion of electron injection occurring within our instrument response (<150 fs) was made by comparison with control data for the dye excited state observed on RuL$_2$(NCS)$_2$-sensitized ZrO$_2$ films.[6] We further note that for the 5 TiO$_2$ films, a low-amplitude, slower (lifetime ∼ 100 ps) component was also observed, however analyses of the amplitude of this component as a function of probe wavelength were inconclusive over its assignment to an electron injection process. We further note that our multiexponential analysis is only intended to provide a crude quantification of the kinetics, it is not clear at present whether the components observed are discrete or result from a distribution of injection time constants.

It is apparent from Figure 3 that the omission of LiClO$_4$ from the electrolyte (electrolyte B) results in a significant retardation of the injection kinetics. This conclusion is further apparent from the transient spectra shown in Figure 4 for these two electrolytes. In the presence of Li$^+$, the spectrum at a time delay of 150 fs (Figure 4a, solid line) is approximately flat between 700 and 800 nm, due to contributions from both the dye excited state (maximum 720 nm) and the dye$^+$(TiO$_2$)$^-$ state (maximum 800 nm) at this time delay. In the absence of Li$^+$, the spectrum at this time delay (Figure 4b, solid line) is dominated by a maximum at 720 nm, indicating that at this time the spectrum results primarily from the dye excited state, consistent with the conclusion of Figure 3 that the absence of Li$^+$ results in a significant retardation of the injection kinetics. Consideration
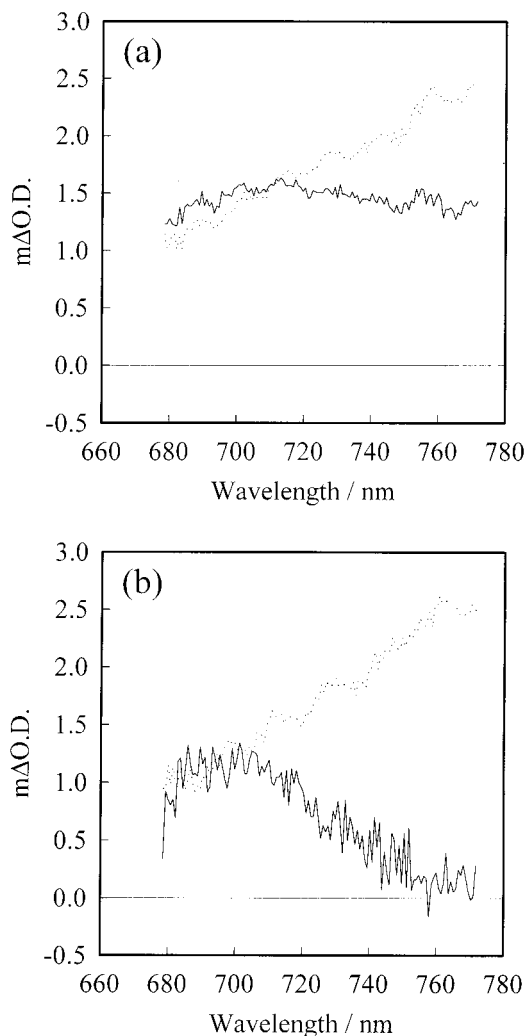
Figure 4. Transient absorption spectra obtained for RuL$_2$(NCS)$_2$-sensitized TiO$_2$ films (a) at time delays of 150 fs (—) and 60 ps (···) in the presence of 0.1 M Li$^+$ (electrolyte A) and (b) at 150 fs (—) and 600 ps (···) in the absence of Li$^+$ (electrolyte B). Other experimental conditions as for Figure 3.

of the spectra obtained at long time delays (dotted spectra) indicate that this retardation does not result in a significant reduction in the final yield of electron injection. For both electrolytes, the spectra at long time delays show an increase in magnitude and red shift of the induced absorption consistent with high overall yields of electron injection. This conclusion was further supported by μs$-$ms data, which also indicated that the dye cation yields in electrolytes A & B were indistinguishable to within ±20%. We conclude it that whereas in the presence of Li$^+$ a significant proportion (∼40%) of the electron injection proceeds in <150 fs, in the absence of Li$^+$ (and any other potential determining ions) electron injection proceeds almost entirely on time scales longer than 150 fs.[33] Global analyses of the data obtained in the absence of Li$^+$ yielded lifetimes (amplitudes) for electron injection of <150 fs (0.075 ± 0.03), 680 ± 80 fs (0.365 ± 0.03), 20 ± 7 ps (0.35 ± 0.03), and >60 ps (0.21 ± 0.03). Comparison of these multiphasic kinetics can be conveniently quantified from the half time for electron injection $t_{50\%}$ (the time for 50% of final electron injection yield to achieved). Such quantification indicates that the omission of Li$^+$ from the electrolyte results in a 7-fold increase in this half time for electron injection.

We now turn the electron injection kinetics as a function of applied electrical bias. Figure 5 shows transient absorption data
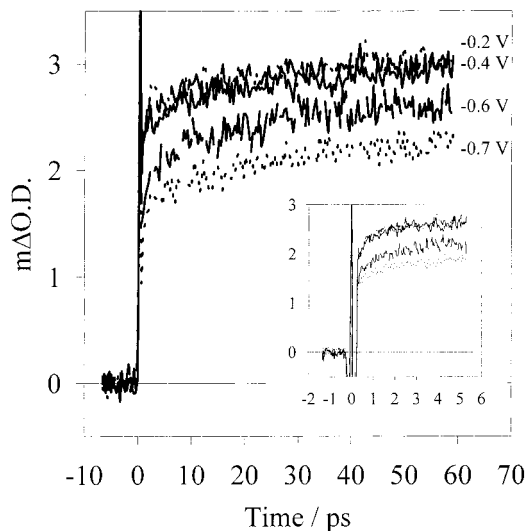

Figure 5. Transient absorption kinetics for RuL$_2$(NCS)$_2$-sensitized TiO$_2$ films collected at a probe wavelength of 760 nm, as a function of electrical potential applied to the TiO$_2$ electrode. Data are shown for potentials between −0.2 and −0.7 V vs Ag/AgCl.

at a probe wavelength of 760 nm for applied potentials between −0.2 and −0.7 V vs Ag/AgCl. Up to −0.4 V the kinetics are largely independent of applied bias. However, at more negative potentials, the kinetics show a significant retardation. Spectra collected at 600 ps (the longest time delay studied) indicated that the yield of electron injection was almost independent of applied bias over this voltage range (only a 15% reduction in yield at −0.7 V relative to that at 0 V). However the kinetics of electron injection, monitored both by the red shift of the photoinduced LMCT absorption and by the magnitude of the cation LMCT absorption showed a significant retardation on all time scales studied. The latter observation is shown in Figure 5 at 760 nm. It is for example apparent that the application of negative biases results in a large reduction in the magnitude of the instrument response limited absorption increase, and therefore in the proportion of electron injection occurring in <150 fs (comparison with control data for dye excited-state absorption obtained for Ru(dcbpy)$_2$(NCS)$_2$ adsorbed to ZrO$_2$ films[6] indicates shifting the potential from −0.2 to −0.7 V reduces the proportion of electron injection occurring in <150 fs from 0.4 to 0.15 ± 0.05). The application of potentials more negative than −0.7 V resulted in a significant reduction in the electron injection yield even at 600 ps, by approximately 50% at −0.8 V. This reduction in injection yield is consistent with excited-state oxidation potential, E_m, for this dye estimated from solution electrochemical studies (−0.75 V vs Ag/AgCl) and from modeling of the data presented here, as detailed below (−0.75 ± 0.05 V). However, it should be noted that the reduction in injection yield observed at such negative potentials (≤ThinSpace−0.8 V) was not fully reversible, suggesting that at such potentials significant dye desorption or degradation may also be occurring. For this reason, quantitative analysis of the data is only considered for potentials up to −0.7 V. As discussed above, comparison of these kinetics can be conveniently quantified as the half time for electron injection, $t_{50\%}$. Figure 6 shows a plot of $t_{50\%}$ as a function of applied bias. It is apparent that the application of −0.7 V results in a ∼25-fold retardation of the kinetics relative to −0.2 V. This observation provides a more direct confirmation of the conclusions of previous studies based on slower time scale measurements of luminescence and/or electron injection yields that the application of negative applied biases retards the electron injection kinetics.[14,34,35] It is

Electron Injection in Dye-Sensitized TiO$_2$ Films
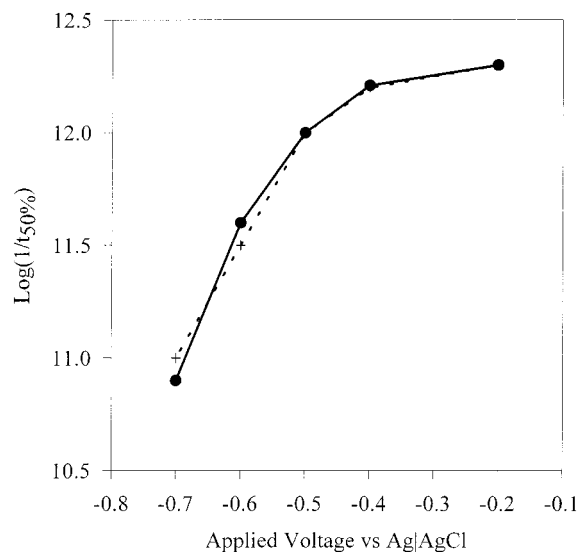
J. Phys. Chem. B, Vol. 105, No. 31, 2001 **7429**

Figure 6. Comparison of the electrical potential dependence of the half time for electron injection, $t_{50\%}$, observed experimentally (+) with that calculated from nonadiabatic electron transfer theory as given by eq 1 (●). Details of the theoretical calculations are given in the Materials and Methods. The best fit to the experimental data, as shown (●) yielded fitting parameters of $E_m = -0.75 \pm 0.05$ V vs Ag/AgCl and $\lambda = 0.25 \pm 0.05$ eV.

moreover consistent with ultrafast stimulated emission studies of dye sensitized SnO$_2$ electrodes.[15]

Discussion

In this paper we have considered the influence of applied electrical potential and the presence of potential determining ions in the electrolyte upon the kinetics of electron injection in RuL$_2$(NCS)$_2$-sensitized nanocrystalline TiO$_2$ films. Both issues are of relevance to the design of photovoltaic devices employing these films. These studies moreover provide further insight into the mechanisms controlling the kinetics of such interfacial electron-transfer processes.

Multiexponential Injection Kinetics. The electron injection kinetics we report here in the presence of Li$^+$ (electrolyte A) at moderate applied potentials are indistinguishable from those we have reported previously for a range of different solvent/ electrolyte conditions in the absence of applied bias.[6,30] We moreover also find essentially the same kinetics for two other sensitizer dyes: zinc and free base tetracarboxyphenyl porphyrins, despite the large differences in excited-state electronic structure of these dyes.[11] In all cases we find the injection kinetics to be multiexponential, requiring a minimum of three components to fit the data. Moreover, we find that in all cases the lifetimes and relative amplitudes of these components were indistinguishable.

The origin of the multiexponential behavior of the observed injection kinetics is at present unclear. Our observation of similar behavior with different sensitizer dyes, and different solvent/ electrolytes suggests that it is associated with a property of the titania films. These films are expected to inhomogeneous, with a significant particle size distribution, multiple exposed crystal faces, and variations in local defect densities. Such inhomogeneities may result in variations in the local density of acceptor states $g(E)$ or the electronic coupling V, thereby giving rise to nonexponential injection kinetics, as has recently been discussed by Lian et al.[26] We further note that our observation of multiexponential kinetics is itself somewhat controversial. Several groups have reported essential monoexponential injec-

tion kinetics for similar 5 titania films,[10,37,38] although more recently other groups have also reported multiexponential injection kinetics.[39]

Comparison with Nonadiabatic Theory: Li$^+$ Effect. Spectroelectrochemical studies of the unsensitized TiO$_2$ films in electrolytes A & B showed that significantly more negative (up to 1 V more negative) electrical biases are required to inject electrons electrically into the TiO$_2$ film in the absence of potential determining ions such as Li$^+$ and H^{+} [17,22] (R. Willis, J.R.D. unpublished data). Such studies therefore indicate that the addition of Li$^+$ ions in the electrolyte results in a positive shift in the density of conduction/trap states, $g(E)$, (i.e., a downward shift in Figure 1) consistent with previous studies.[22] It is unclear whether this net shift results from a shift in the energy of all titania conduction band states or the introduction by Li$^+$ of additional states within the band gap. Not withstanding this ambiguity, from eq 1 it is apparent that the net shift in $g(E)$ to less negative energies induced by Li$^+$ is expected to result in an acceleration in the injection kinetics, in agreement with our experimental observations. It can be concluded that the dependence of the electron injection kinetics upon electrolyte composition is at least qualitatively consistent with the predictions of eq 1.

A more quantitative analysis of the electrolyte dependence of the injection kinetics is not possible at present. For example, it has been suggested that variations in electrolyte composition may also result in variations, albeit probably smaller, in the dye midpoint potential E_m.[23] We further note that the sensitizer dye employed here includes 4 carboxylic acid groups, resulting in a significant proton concentration in the electrochemical cell during the laser experiments and complicating quantitative comparison with spectroelectrochemical data obtained for unsensitized films.

The dependence of the injection kinetics upon Li$^+$ concentration we observed here is qualitatively consistent with the conclusion of previous studies based upon determination of the yield of electron injection as a function of concentration of potential determining ions.[25] The dependence we observe here is relatively modest (only a factor of 7), insufficient to result in significant modulation of the injection yield under our experimental conditions (the dye excited-state decay time is 3−20 ns[6]). We note, however, that in experiments conducted under more rigorously aprotic conditions, and in particular with an aprotic sensitizer dye, the yield of electron injection has also been reported to be sensitive to Li$^+$ concentration.[25]

Comparison with Nonadiabatic Theory: Effect of Applied Electrical Potential. Figure 6 compares the experimentally observed dependence of the electron injection kinetics upon applied bias with that calculated by eq 1. Full details of the calculations are given in the Materials and Methods. It is apparent that the fit to the data employing eq 1 is in good agreement with experiment. Moreover the value of the dye excited-state oxidation potential obtained from this fit, −0.75 ± 0.05 V vs Ag/AgCl, is in good agreement with that obtained from solution phase electrochemical studies. The value of the reorganization energy obtained, 0.25 eV, is typical of molecular reorganization energies for electron-transfer reactions on this time scale. It can be concluded that, at least for the experimental system studied here, the nonadiabatic description of interfacial electron transfer as detailed by eq 1 is in good agreement with our experimental observations.

We note that the calculations employed here consider only the half-time for electron injection, and do not take account of the distribution of time constants obtained from multiexponential

analyses at a single bias. Our analysis therefore assumes the origin of the nonexponentiality of the kinetics is bias independent. This assumption is supported by our observation that the injection kinetics appears to be retarded by the applied bias over all time scales and moreover seems reasonable to us given the likely origins of the nonexponential kinetics (variations in electronic coupling or local density of states).

The nonadiabatic theory we have employed here assumes the nuclear motions of dye excited state reach thermal equilibrium with the environment prior to electron injection. Moreover the value of E_m obtained here indicates that electron injection proceeds following electronic relaxation of the dye to its lowest energy excited state. The agreement we obtain between experiment and theory implies both assumptions are essentially valid. This agreement is consistent with the half times we find for electron injection (≥ 500 fs), which are significantly slower than typical nuclear/solvent reorganization times and with electronic relaxation times within exited state manifold of such ruthenium bipyridyl dyes (<100 fs[6,40]). We note however that several groups have reported fast, < 100 fs, electron injection kinetics for other 5 metal oxide films, and discussed such kinetics both in terms of adiabatic electron transfer theory, and "hot" electron injection from unrelaxed dye excited states.[5,7,10,12] Given the complexity of our observed electron injection kinetics, it is possible that the fast (<150 fs) phase of injection, which accounts for up to 40% of the total injection yield at moderate potentials, may correspond to such processes. However such considerations are not necessary to account for the overall behavior of the electron injection kinetics of the $RuL_2(NCS)_2$-sensitized TiO_2 films studied in this paper. We further note that this <150 fs phase of electron injection was also observed to be bias dependent, consistent with its inclusion in our numerical analysis.

The calculations employed in Figure 6 do not take account of electrostatic repulsions arising from the increased in electron occupancy of each TiO_2 nanoparticle induced by the negative applied bias. Spectroelectrochemical data suggests that -0.7 V results in an increase of electron occupancy per nanoparticle of approximately 3 electrons. However the high dielectric constant TiO_2 (~ 100[31,41,42]), indicates the repulsion energy for two electrons separated by 10 nm within a nanoparticle is only of the order of only 1 mV.[43] Furthermore screening of the electron charge is likely to arise from surface adsorption/intercalation of positive ions from the electrolyte. On this basis, such electrostatic repulsions can be safely neglected for the electron occupancies considered here. This conclusion is supported by the good agreement we obtain between experiment and theory without consideration of such interactions.

We find that the application of more extreme potentials results in a reduction in the yield of electron injection and an associated increase in long-lived excited states, which are only partially/slowly reversible. These observations are consistent with the recent quartz microbalance study of Lemon & Hupp[16] which concluded that the application of negative potentials to such 5 nanocrystalline TiO_2 films can induce desorption of the sensitizer dye.

Implications for the Function of Photoelectrochemical Solar Cells. We have demonstrated here that the rate of electron injection is sensitive both to the electrolyte composition and electrical bias applied. However, in both cases the magnitude of the dependence is relatively modest, compared for example to the much larger dependency upon these parameters observed for the charge recombination dynamics.[27] Exclusion of Li^+ from the electrolyte resulted in a 7-fold retardation of the injection

kinetics, while the application of -0.7 V versus Ag/AgCl resulted in a 25-fold retardation. Given the midpoint potential of the I_3^-/I^- redox couple typically employed in functioning devices, the open circuit potential V_{oc} of such devices corresponds to an applied potential in our 3 electrode electrochemical cell of approximately -0.5 V. At this potential, the $t_{50\%}$ for electron injection, is ~ 2 ps, only a factor of 4 slower than that observed in the absence of applied potential. It can be concluded that the half time for electron injection even at V_{oc} is likely to be approximately 3 orders of magnitude faster than the dye excited-state lifetime (3−20 ns), resulting in a near unity injection yield. While clearly caution most be taken in extrapolating from the experiments reported here to a photoelectrochemical solar cell operating under illumination, our observations do suggest that, at least in the presence of potential determining ions such as Li^+ in the electrolyte, the bias dependence of the injection kinetics is unlikely to play a key role in limiting the energy conversion efficiency of such devices.

We have reported elsewhere[11,30] that the multiexponential kinetics we observe for electron injection are independent of the solvation and electronic structure of the sensitizer dye (for a limited range of dyes), from which we conclude that the multiple time constants we observed result from heterogeneities in the energetics/surface structure of the nanocrystalline TiO_2 films. We find here that, under potentiostatic control of the TiO_2 Fermi level, the electron injection kinetics are dependent upon both the presence of potential determining ions in the electolyte and the applied potential. These dependencies can be explained as deriving from variations in, respectively, the energy and occupancy of the titania electronic density of states available for electron injection. This observation further emphasizes the importance of the semiconductor film in influencing the kinetics of interfacial electron transfer in this system.

References and Notes

(1) O'Regan, B.; Grätzel, M. *Nature* **1991**, *353*, 737−739.

(2) Hagfeldt, A.; Gratzel, M. *Acc. Chem. Res.* **2000**, *33*, 269−277.

(3) Schmickler, W. *Interfacial Electrochemistry*; Oxford University Press: Oxford, 1996.

(4) Rehm, J. M.; Mclendon, G. L.; Nagasawa, Y.; Yoshihara, K.; Moser, J.; Grätzel, M. *J. Phys. Chem.* **1996**, *100*, 9577−9578

(5) Burfeindt, B.; Hannappel, T.; Storck, W.; Willig, F. *J. Phys. Chem.* **1996**, *100*, 16463−16465.

(6) Tachibana, Y.; Moser, J. E.; Grätzel, M.; Klug, D. R.; Durrant, J. R. *J. Phys. Chem.* **1996**, *100*, 20056−20062.

(7) Huber, R.; Spörlein, S.; Moser, J. E.; Grätzel, M.; Wachtveitl, J. *J. Phys. Chem. B* **2000**, *104*, 8995−9003.

(8) Hilgendorff, M.; Sundström, V. *J. Phys. Chem. B* **1998**, *102*, 10505−10514.

(9) Martini, I.; Hodak, J. H.; Hartland, G. V. *J. Phys. Chem. B* **1998**, *102*, 9508−9517.

(10) Asbury, J. B.; Ellingson, R. J.; Ghosh, H. N.; Ferrere, S.; Nozik, A. J.; Lian, T. *J. Phys. Chem. B* **1999**, *103*, 3110−3119.

(11) Tachibana, Y.; Haque, S. A.; Mercer, I. P.; Klug, D. R.; Durrant, J. R. *J. Phys. Chem B* **2000**, *104*, 1198−1205.

(12) Ramakrishan, S.; Willig, F. *J. Phys. Chem B* **2000**, *104*, 68−77.

(13) Smith, B. B.; Nozik, A. J. *J. Phys. Chem. B* **1997**, *101*, 2459−2475.

(14) Kamat, P. V.; Bedja, I.; Hotchandani, S.; Patterson, L. K. *J. Phys. Chem.* **1996**, *100*, 4900−4908.

(15) Iwai, S.; Hara, K.; Murata, S.; Katoh, R.; Sugihara, H.; Arakawa, H. *J. Chem. Phys.* **2000**, *113*, 3366−3373.

(16) Lemon, B. I.; Hupp, J. T. *J. Phys Chem. B* **1999***, 103*, 3797−3799.

(17) Rothenberger, G.; Fitzmaurice, D.; Grätzel, M. *J. Phys. Chem.* **1992**, *96*, 5983−5986.

(18) Boschloo, G.; Fitzmaurice, D. *J. Phys. Chem.* **1999**, *103*, 7860−7868.

(19) Duffy, N. W.; Peter, L. M.; Rajapakse; R. M. G.; Wijayantha, K. G. U. *Electrochem. Commun.* **2000**, *2*, 658−662.

(20) Willis, R. L.; Olson, C.; O'Regan, B.; Lutz, T.; Nelson, J.; Durrant, J. R., in preparation.

(21) Kay, A.; Grätzel, M. *J. Phys. Chem.* **1993**, *97*, 6272−6277.

(22) Redmond, G.; Fitzmaurice, D. *J. Phys. Chem.* **1993**, *97*, 1426−1430.

(23) Zaban, A.; Ferrere, S.; Gregg, B. A. *J. Phys. Chem. B* **1998**, *102*, 452−460.

(24) Yan, S. G.; Hupp, J. T. *J. Phys. Chem. B* **1997**, *101*, 1493−1495.

(25) Thompson, D. W.; Kelly, C. A.; Farzad, F.; Meyer, G. J. *Langmuir* **1999**, *15*, 650−653.

(26) Haque, S. A.; Tachibana, Y.; Klug, D. R.; Durrant, J. R. *J. Phys. Chem. B* **1998**, *102*, 1745−1749.

(27) Haque, S. A.; Tachibana, Y.; Willis, R.; Moser, J. E.; Grätzel, M.; Klug, D. R.; Durrant, J. R. *J. Phys. Chem. B* **2000**, *104*, 538−547.

(28) Nelson, J. *Phys. Rev. B* **1999**, *59*, 15374−15380.

(29) Nelson, J.; Haque, S. A.; Klug, D. R. Durrant, J. R. *Phys. Rev. B*, in press.

(30) Durrant, J. R.; Tachibana, Y.; Mercer, I. P.; Moser, J. E.; Grätzel, M.; Klug, D. R. *Z.Phys. Chem.* **1999**, *212*, S. 93−98.

(31) Cao, F.; Oskam, G.; Searson, P. C.; Stipkala, J. M.; Heimer, T. A.; Farzad, F.; Meyer, G. J. *J. Phys. Chem.* **1995**, *99*, 11974−11980.

(32) Moser, J. E.; Noukakis, D.; Bach, U.; Tachibana, Y.; Klug, D. R.; Durrant, J. R.; Humphry-Baker, R.; Grätzel, M. *J. Phys. Chem. B* **1998**, *102*, 3649−3650.

(33) Prolonged (>5 min) excitation of one spot of the TiO$_2$ film in electrolyte B resulted in a gradual, reversible acceleration of the injection kinetics; the origin of this kinetic change is currently unclear.

(34) Hoyer, P.; Weller, H. *J. Phys. Chem.* **1995**, *99*, 14096−14100.

(35) O'Regan, B.; Moser, J.; Grätzel, M. *J. Phys. Chem.* **1990**, *94*, 8720−8726.

(36) Asbury, J. B.; Wang, W.; Lian, *J. Phys. Chem. B* **1999**, *103*, 6643−6647.

(37) Ellingson, R. J.; Asbury, J. B.; Ferrere, S.; Ghosh, H. N.; Sprague, J.; Lian, T.; Nozik, A. J. *J. Phys. Chem. B* **1998**, *102*, 6455−6458.

(38) Hannappel, T.; Burfeindt, B.; Storck, W.; Willig, F. *J. Phys. Chem. B* **1997**, *101*, 6799−6802.

(39) Benkö, G.; Hilgendorff, M.; Yartsev, A. P.; Sundström, V. *J. Phys. Chem. B* **2001**, 967−974.

(40) Damrauer, N. H.; Cerullo, G.; Yeh, A.; Boussie, T. R.; Shank, C. V.; McCusker, J. K. *Science* **1997**, *275*, 54−57.

(41) Krol, R. V.; Goossens, A.; Schoonman, J. *J. Electrochem. Soc.* **1997**, *144*, 1723−1727.

(42) Most reported values of dielectric constants for anatase nanocrystalline TiO$_2$ films significantly vary from 100 to 180; however, much lower values of <60 were also reported.

(43) This calculation neglects screening of the electronic charge by the electrolyte, and is therefore an upper limit for the interaction energy.